Chapter 3: The effect of anthracene-polyamine conjugates on intra-erythrocytic *P. falciparum* parasites.

3.1 Introduction

Polyamine metabolism has been proposed as a target for the treatment of proliferative diseases such as cancer, as well as microbial and parasitic infections (Heby *et al.*, 2003). However, DFMO, used to treat West African sleeping sickness (caused by *T. brucei gambiense*) (Bacchi *et al.*, 1990; Casero and Woster, 2009), is the only polyamine metabolism antagonist that has shown clinical usefulness. The clinical failure of most of the polyamine biosynthesis inhibitors (Paridaens *et al.*, 2000; Seiler *et al.*, 1998) is often attributed to compensatory mechanisms that maintain the intracellular polyamine pool (Müller *et al.*, 2001; Wallace *et al.*, 2003). This includes the up-regulation of polyamine uptake mechanisms (Alhonen-Hongisto *et al.*, 1980; Boncher *et al.*, 2007). DFMO causes cytostatic growth arrest in most cancerous cells (Wallace *et al.*, 2003) as well as in parasitic organisms such as intra-erythrocytic *P. falciparum* parasites (Assaraf *et al.*, 1987b). However, in polyamine transport deficient cancerous cell lines, DFMO elicits a cytotoxic response since these cells are unable to overcome the polyamine-depletion by the uptake of extracellular polyamines (Palmer *et al.*, 2009; Seiler, 1991; Wallace and Fraser, 2004).

The disappointing results obtained with polyamine biosynthesis inhibitors alone has prompted a shift in focus from developing compounds that target the biosynthetic enzymes, to producing polyamine-like molecules (polyamine analogues) (Casero and Woster, 2009; Palmer and Wallace, 2010). These compounds have sufficient similarity in structure to the polyamines to gain entry into the cell via polyamine uptake pathways, but once inside cells, act as polyamine antagonists (Palmer and Wallace, 2010; Wallace and Niiranen, 2007; Wallace and Fraser, 2003). 'Polyamine mimetics' are defined as polyamine analogues that decrease cellular growth without causing polyamine depletion, by occupying normal polyamine binding/effector sites (e.g. DNA) but failing to produce the normal biological actions of the endogenous polyamines (Wallace and Fraser, 2004; Wallace *et al.*, 2003).

'Polyamine anti-metabolites', in contrast, result in cell growth inhibition and a reduction in polyamine levels through either biosynthesis inhibition and/or induction of polyamine catabolism and export (Wallace and Fraser, 2004; Wallace *et al.*, 2003). Polyamine analogues have been synthesised with modifications including simple conjugation of additional moieties (Phanstiel *et al.*, 2000), both symmetrical (Bergeron *et al.*, 1988) and unsymmetrical (Saab *et al.*, 1993) terminally alkylated polyamines and structural analogues of the polyamines (reviewed extensively elsewhere (Casero and Woster, 2001, 2009; Palmer and Wallace, 2010).

Polyamine analogues have also been designed to inhibit polyamine uptake itself (Palmer and Wallace, 2010). For instance, the polyamine analogue, *trans*-1,4-diamino-2-butene, inhibits *E. coli* putrescine transporters PotE and PotFGHI by 50%, (200 and 50 µM, respectively) (Kashiwagi *et al.*, 2000). Spermine conjugated to lysine is an effective polyamine transport inhibitor in MDA-MB-231 breast carcinoma cells (Graminski *et al.*, 2002), whereas spermine heterocyclically conjugated to benzazepine effectively inhibits polyamine transport (Ki 0.12 µM) in L1210 cells (Tomasi *et al.*, 2010). A polyamine analogue, 1,4-diamino-2-butanone (DAB), exhibited dose-dependent inhibition of *in vitro* proliferation in *Giardia lamblia* (Maia *et al.*, 2008), *Tritrichomonas foetus* (Reis *et al.*, 1999), *Trichomonas vaginalis* (Alvarez-Sanchez *et al.*, 2008) as well as *T. cruzi* epimastigotes (Menezes *et al.*, 2006). For the latter, it was postulated that DAB binds to a putrescine transporter at the cell surface, thus leading to putrescine depletion as well as oxidative stress and cell death (Menezes *et al.*, 2006).

The broad specificity of certain polyamine uptake systems allows the uptake of polyamine analogues (Palmer *et al.*, 2009; Phanstiel *et al.*, 2007; Wang *et al.*, 2003a). This promiscuity has led to strategies being proposed whereby polyamine moieties conjugated to e.g. toxic cargo would enhance the delivery of this cargo into cells through the polyamine uptake system (Palmer and Wallace, 2010; Phanstiel *et al.*, 2007). Several terminally alkylated polyamine analogues have been investigated where the cargo-polyamine spacer, the size of the N^1-substituent cargo and the degree of N^1-substitution all influenced the uptake of these analogues (Breitbeil *et al.*, 2006; Kaur *et al.*, 2008). A range of anthracene-polyamine conjugates has been designed to utilise polyamine uptake mechanisms in mammalian cells (L1210 cells and CHO cells) to deliver the toxic anthracene cargo (as DNA intercalating agent) to these cells (Kaur *et al.*, 2008; Phanstiel *et al.*, 2007; Wang *et al.*, 2003a). Anthracene-conjugated polyamines had an 150-fold higher cytotoxicity in CHO cells

compared to alkylated (e.g. propyl or butyl conjugated for solubility) anthracene derivatives (Cullis *et al.*, 1999; Tsen *et al.*, 2008; Wang *et al.*, 2003a). Additionally, these anthracene-polyamine conjugates have shown selectivity for the mammalian polyamine transport system(s) with enhanced toxicity in CHO cells compared to polyamine transport deficient CHO-MG mutant cells (Covassin *et al.*, 1999; Delcros *et al.*, 2002; Phanstiel *et al.*, 2000; Wang *et al.*, 2001). Recently, an anthracene-putrescine conjugate was shown to enter HL-60 cells through the polyamine uptake mechanism, followed by apoptotic cell death caused by the polyamine moiety as well as the attached anthracene cargo (Palmer *et al.*, 2009).

The work described in this chapter investigates the effect of selected anthracene-polyamine conjugates (Fig. 3.1) on intra-erythrocytic *P. falciparum* parasites. Anthracene was conjugated to various polyamines, all with different combinations of carbon-backbones. As such, Ant-4 was produced as a putrescine conjugate (Ant-CH_2-NH-$(CH_2)_4$-NH_2); Ant-44 as a homospermidine conjugate (Ant-CH_2-NH-$(CH_2)_4$-NH-$(CH_2)_4$-NH_2); Ant-444 as a homospermine conjugate (Ant-CH_2-NH-$(CH_2)_3$-NH-$(CH_2)_4$-NH-$(CH_2)_3$-NH_2); and 44-Ant-44 as a bis-homospermidine conjugate (NH_2-$(CH_2)_4$-NH-$(CH_2)_4$-NH-CH_2-Ant-CH_2-NH-$(CH_2)_4$-NH-$(CH_2)_4$-NH_2) (Liao *et al.*, 2009; Phanstiel *et al.*, 2000).

Ant-4

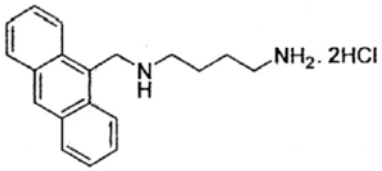

Ant-44

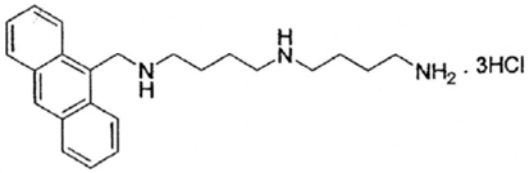

Ant-444

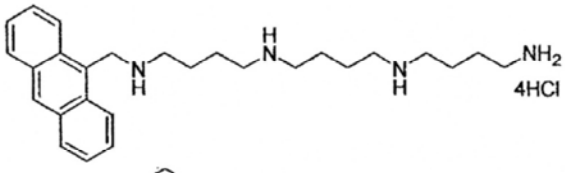

44-Ant-44

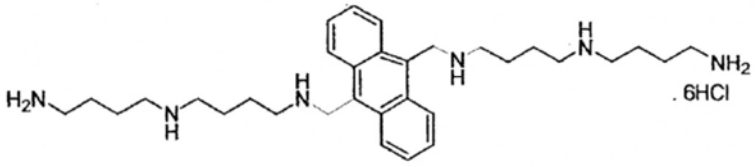

Figure 3.1: Structures of anthracene-polyamine conjugates. Adapted from (Liao *et al.*, 2009). Ant-4 is a putrescine conjugate; Ant-44 is a homospermidine conjugate; Ant-444 is a homospermine conjugate; and 44-Ant-44 is a bi-conjugated homospermidine conjugate.

3.2 Materials and methods

3.2.1 *In vitro* cultivation of intra-erythrocytic *P. falciparum* parasites

P. falciparum (3D7) parasites were maintained as described in Chapter 2, section 2.3.

3.2.2 Parasite proliferation assays

The *in vitro* anti-plasmodial activity of the compounds were determined by using the malaria SYBR Green I fluorescence assay as has been described (Bennet *et al.*, 2004; Smilkstein *et al.*, 2004) with minor modifications. The SYBR green I fluorescence assay relies on the fluorescent dye (SYBR Green I) intercalating into DNA, which correlates DNA levels directly with parasite growth. *In vitro* ring-stage *P. falciparum*-infected RBC cultures (1% haematocrit, 1% parasitaemia) were incubated with Ant-4, Ant-44, Ant-444 and 44-Ant-44 (Wang *et al.*, 2003b), all dissolved in 1xPBS and diluted to specific concentrations in complete *P. falciparum* culture medium, with chloroquine disulphate used as a positive control (0.5 µM) or vehicle (1xPBS) as negative control. iRBC cultures (200 µl) were grown statically at 37˚C for 96 hrs in 96-well plates, after which the cells were re-suspended and combined in equal volumes (100 µl each) with SYBR Green I lysis buffer (0.2 µl/ml 10 000x SYBR Green I Invitrogen, Inc; 20 mM Tris, pH 7.5; 5 mM EDTA; 0.008% (w/v) saponin; 0.08% (v/v) Triton X-100) and fluorescence measured after an 1 hr incubation at 37˚C using a Fluoroskan Ascent FL microplate fluorometer (Thermo Scientific, excitation at 485 nm and emission at 538 nm). The data, after subtraction of background (chloroquine disulphate treated iRBCs, no parasite growth) were expressed as percentage of untreated control to determine cell proliferation and averaged from at least 3 independent experiments (± S.E.), unless where otherwise stated.

3.2.3 Determination of anthracene-polyamine uptake into iRBCs

Deconvolution fluorescent microscopy was used to visualise uptake of Ant-4 into iRBCs. *In vitro* ring-stage *P. falciparum* (3D7) cultures at a 5% haematocrit and ~5% parasitaemia were incubated for 24 hrs to allow the parasites to develop to the trophozoite stage before

addition of Ant-4 (100 µM) for 1 hr at 37°C. Subsequently, 200 µl of these iRBC cultures were centrifuged at 500xg, washed in 1xPBS and re-suspended in 200 µl of a 1/1000-dilution SYBR Green I (10 000x SYBR Green I Invitrogen, Inc) in 1xPBS at 37°C for 30 min. Images were captured with a Zeiss Axio Observer Z.1, with an Andor iXon EMCCD camera and Andor iQ imaging software (Andor Technology, Ireland) or a Nikon Eclipse Ti with an Andor iXon EM+EMCCD camera (Andor Technology) using µManager open source imaging software (http://valelab.ucsf.edu/) and analysed with ImageJ (Abramoff *et al.*, 2004). Nuclei were visualised using a FITC filter (excitation band pass (BP) 470/40 and emission BP 525/50; or excitation BP 500/24 and emission BP 542/27, respectively) and the anthracene moiety was visualised with a DAPI filter (excitation 365 nm and emission BP 445/50 or excitation BP 377/50 and emission BP 447/60). Three independent drug treatments were performed.

Uptake of Ant-4 into RBCs, iRBCs and isolated *P. falciparum* trophozoites was also investigated using an alternative approach. RBCs (5% haematocrit) or ring stage iRBCs cultures (5% haematocrit and ~5% parasitaemia) were pre-treated with DFMO (1 mM) for 24 hrs to deplete intracellular polyamine levels (Assaraf *et al.*, 1987b) before incubating 200 µl of either RBCs cultures or now trophozoite-stage iRBCs cultures with Ant-4 (400 µM) for 60 min at 37°C. Isolated *P. falciparum* trophozoites were obtained with saponin lysis as described in section 2.2.2 (Saliba *et al.*, 1998). The RBCs, iRBCs or isolated parasites described above were subsequently centrifuged, washed and re-suspendend in 1xPBS (750 µl). Fluorescence was measured with a DAPI filter (BP 450/40 emission) using a BD FACS ARIA (BD Biosciences) equipped with a violet laser with excitation at 407 nM. Data from at least 10^5 cells from three independent experiments were analysed with Cyflogic v1.2.1 (CyFlo Ltd).

3.2.4 Determination of the effects of polyamine conjugates on putrescine uptake into isolated *P. falciparum* trophozoites

The effects of Ant-4, Ant-44, Ant-444 and 44-Ant-44 on [^{3}H]putrescine uptake into isolated *P. falciparum* trophozoites were investigated as described in sections 2.2.2 and 2.2.3. The reaction buffer (125 mM NaCl, 5 mM KCl, 20 mM glucose, 25 mM HEPES and 1 mM $MgCl_2$, pH 7.1) was supplemented with 1 µCi/ml [^{3}H]putrescine (Amersham) and anthracene-polyamine conjugates (1 mM). The uptake reactions were initiated by the addition of equal volumes of reaction buffer and the isolated trophozoite cell suspension to reach final

concentrations of 0.5 µCi/ml [^{3}H]putrescine and 500 µM each of Ant-4, Ant-44, Ant-444 and 44-Ant-44. These concentrations are 10-fold lower than was used for the metabolite inhibition assays (section 2.3.2.5) due to limited compound availability. Following a 30 min incubation at 37°C, the uptake reactions were terminated and the uptake of the radiolabel determined as described in section 2.2.3. Data were represented as percentage of control (± S.E.) averaged from four independent experiments.

3.2.5 Determination of the effect of polyamines on Ant-4 uptake into intra-erythrocytic *P. falciparum* trophozoites

The effects of putrescine and spermidine on Ant-4 uptake into isolated *P. falciparum* trophozoites were investigated as follows: ring-stage iRBC cultures (5% haematocrit and ~5% parasitaemia) were pre-treated with DFMO (1 mM) as described in section 3.2.3 for 24 hrs to deplete intracellular polyamine levels (Assaraf *et al.*, 1987b) before washing the cells, followed by re-suspending the cells to (5% haematocrit and ~5% parasitaemia), and incubating 200 µl of the now trophozoite-stage iRBCs cultures with Ant-4 (400 µM) with and without putrescine dihydrochloride or spermidine trihydrochloride (500 µM) for 60 min at 37°C. A 50 µl aliquot of the iRBC culture (5% haematocrit and ~5% parasitaemia), was sampled and the cells were washed and re-suspended in 1xPBS (750 µl). Fluorescence was measured with a DAPI filter (BP 450/40 emission) using a BD FACS ARIA (BD Biosciences) equipped with a violet laser with excitation at 407 nM. Data from at least 10^5 cells from three independent experiments were analysed with Cyflogic v1.2.1 (CyFlo Ltd). Gating was performed based on uninfected RBCs to obtain the iRBC population.

3.2.6 Measurement of intracellular polyamine levels in intra-erythrocytic *P. falciparum* trophozoites

Intracellular polyamine levels following Ant-4 treatment were measured as has been described by Becker *et al.* (2010). In brief, synchronised *P. falciparum* (3D7) ring-stage cultures (5% haematocrit, 15% parasitaemia) were incubated with Ant-4 (2xIC_{50}) for 24 hrs before the cells were harvested and washed four times in 1xPBS. The polyamines were extracted from the cell pellet with an equal volume of 5% (v/v) perchloric acid (PCA), followed by 12 hrs incubation at 4°C. The acid-insoluble components were removed by centrifugation at 16 000xg for 10 min at 4°C. NaOH (2 M, 1 ml) was added to the polyamine-PCA extracts, followed by benzoylation with 1:100 v/v benzoyl chloride (Sigma-

Aldrich) for 30 min at 37°C. The benzoylated polyamines were extracted with chloroform, dried under a nitrogen stream and re-constituted in 500 µl of 60% MeOH. HPLC analysis was performed using a 250×4.0 mm Luna C18 5 µm reverse-phase column and a WATERS System under isocratic solvent conditions (60% MeOH:ddH_2O) (Becker *et al.*, 2010). The Empower 2 Software (2006 ed., Waters Corporation) with Apex™ Trac functionality was used for peak integration. Data were expressed as a percentage of control (± S.E.) and averaged from four independent experiments.

3.2.7 Cytotoxicity and cell viability measurements

Cytotoxicity assays were performed using the CellTiter 96® Aq_{ueous} One Solution Cell Proliferation assay (Promega, USA) according to the manufacturer's instructions. Cell viability is indicated by the reduction of the tetrazolium compound MTS [3-(4,5-dimethylthiazol-2-yl)-5-(3-carboxymethoxyphenyl)-2-(4-sulfophenyl)-2H-tetrazolium, inner salt] to a coloured formazan product by metabolically active cells (Cory *et al.*, 1991). Ring-stage iRBC cultures (0.5% haematocrit, 25% parasitaemia) were exposed to Ant-4 (1x and 5xIC_{50}), chloroquine disulphate (0.5 µM, positive control) or vehicle (1xPBS, negative control) at 37°C for 24 hrs. The relatively high parasitaemia of 25% was needed to ensure sufficient parasite cells for the cytotoxicity assay. By reducing the haematocrit, the overall cell-density was reduced to ensure pH maintenance and a sufficient supply of nutrients. iRBCs were subsequently washed and re-suspended in culture media to 1% haematocrit and 25% parasitaemia to ensure that sufficient cells were present to obtain detectable signals. CellTiter 96® Aq_{ueous} One Solution (20 µl) was added to 100 µl of the above trophozoite cell suspension and incubated at 37°C for 4 hrs in a gaseous environment of 90% N_2, 5% O_2, and 5% CO_2 before measuring the absorbance at 492 nm with a Multiskan Ascent scanner (Thermo labsystems). Cell counts were performed using an improved Neubauer cell counting chamber. Data were expressed as a percentage of control and averaged (± S.E) for four independent experiments. Additionally, parasite proliferation was monitored over 96 hrs following treatment of ring-stage parasites (1% haematocrit, 1.5% parasitaemia) with Ant-4 (3xIC_{50}) in the presence and absence of 1 mM putrescine dihydrochloride using Giemsa-stained smears. These were prepared every 24 hrs and visualised with a light microscope to determine the parasitaemia by counting at least 10 fields of >100 cells each.

3.2.8 Determination of oxidative stress

Intracellular glutathione was measured using the GSH-Glo™ Glutathione Assay (Promega). Luciferin is produced in the presence of reduced glutathione and a luminescence signal is generated via a coupled luciferase reaction. Intra-erythrocytic ring-stage cultures (0.5% haematocrit, 25% parasitaemia) were incubated with Ant-4 (1xIC_{50}), or vehicle (1xPBS, positive control) at 37˚C for 24 hrs. The iRBC cultures were then centrifuged, washed and re-suspended in 1xPBS to 1% haematocrit and 25% parasitaemia. GSH-Glo™ reagent (100 µl) was added to 100 µl of the above cell suspension, which was incubated for 30 min at room temperature, before adding equal volumes of the cell/GSH-Glo™ reagent mix to the Luciferin Detection reagent. Following a 10 min incubation, the luminescence was measured using an Infinite® F500 multimode microplate reader (Tecan Group Ltd.) with an integration time of 1000 ms. A range of glutathione standards were prepared and measured as above to generate a standard curve for the determination of the amount of reduced glutathione in the samples. Data were averaged (± S.E.) from four independent experiments.

In addition, DCFDA (2'-7'-dichloro-dihydrofluorescein diacetate) was used to measure the production of reactive oxygen species (ROS), particularly H_2O_2 levels, in intra-erythrocytic *P. falciparum* cultures treated with Ant-4. DCFDA is non-fluorescent, but upon oxidation by ROS and peroxides converts to the fluorescent derivative DCF. Intra-erythrocytic ring-stage cultures (5% haematocrit, 5% parasitaemia) were incubated for 24 hrs with Ant-4 (1xIC_{50}) at 37˚C or with H_2O_2 as a positive control for ROS for 30 min. The treated and untreated iRBC cultures (5% haematocrit, 5% parasitaemia, 100 µl) were subsequently incubated with 20 µM DCFDA for 20 min at 37°C. Additionally, iRBC cultures (5% haematocrit, 5% parasitaemia, 100 µl) were incubated with 20 µM H_2O_2 immediately prior to the DCFDA staining described above. Fluorescence was measured in the FITC channel (FL1) on a FACS FC500 System (Beckman Coulter) equipped with an air-cooled argon laser with 488 nm excitation. Data from at least 10^6 cells were analysed with FlowJo v9.1 (Tree Star).

3.2.9 Investigation of DNA levels and DNA replication

DNA levels were monitored over 96 hrs following treatment of ring-stage iRBC cultures (1% haematocrit, 1.5% parasitaemia) with Ant-4 (3xIC_{50}) using an adapted SYBR green I Fluorescence assay. SYBR Green I fluoresce due to the intercalation of the dye into DNA thereby allowing the measurement of relative DNA levels (Bennet *et al.*, 2004). Equal

volumes (100 µl) of these iRBC cultures were combined with the SYBR Green I lysis buffer as described above (section 3.2.2) and the fluorescence was measured after a 1 hr incubation at 37˚C, using a Fluoroskan Ascent FL microplate fluorometer (Thermo Scientific, excitation at 485 nm and emission at 538 nm). The background fluorescence was subtracted and the data averaged ± S.E. from three independent experiments.

To monitor DNA replication as well as nuclear division, ring-stage iRBCs (1% haematocrit, ~5% parasitaemia) were incubated with Ant-4 (1xIC_{50} and 5xIC_{50}), or vehicle (1xPBS, negative control) at 37˚C for 24 hrs. iRBC cultures (100 µl) were used either fresh or fixed with 1 ml of 0.025% glutaraldehyde for 45 min and kept at 4°C until assayed. These cells were washed, and re-suspended in 20 µl 1:1000 SYBR Green I for 30 min in the dark at room temperature to stain the parasite's DNA, washed four times with 1xPBS and analysed on a FACS FC500 System (Beckman Coulter) equipped with an air-cooled argon laser with 488 nm excitation. At least 10^5 cells were analysed for each sample with fluorescence emission collected in the FL-1 channel (FITC signal). FlowJo v9.1 (Tree Star) was used to analyze the data. Experiments were performed in duplicate for three independent experiments. Gating was performed based on uninfected RBCs to obtain the iRBC population. Within this population, gating was subsequently also performed for peaks corresponding to iRBCs containing parasites with 1 nucleus (1N, either rings or trophozoite forms), or multiple nuclei (2N, 3N, 4N or >4N) corresponding to late-stage schizont parasites.

3.2.10 Determination of mitochondrial membrane potential

The effect of Ant-4 treatment of intra-erythrocytic *P. falciparum* parasites on the mitochondrial membrane potential ($\Delta\psi m$) was determined with the dye JC-1 (5,5',6,6'-tetrachloro-1,1',3,3'-tetraethylbenzimidazolylcarbocyanine iodide, Biotium). JC-1 fluoresces red (FL2 signal, DAPI filter) in normal cells and green (FL1 signal, FITC filter) in cells that have undergone a loss of $\Delta\psi m$. Ring-stage *P. falciparum* (3D7) cultures (1% haematocrit, ~5% parasitaemia) were incubated with Ant-4 (1xIC_{50}) at 37˚C for 24 hrs. Subsequently, 10 µl of the untreated and treated iRBC cultures were washed in 1xPBS and the cells re-suspended in 1xJC-1 solution as per the manufacturer's instructions, incubated at 37˚C for 15 min in the dark, washed twice in 1xPBS and analysed by flow cytometry as described above (section 3.2.8).

3.2.11 Statistical analysis

Statistical significance was determined with a two-tailed t-test using the Graphpad Instat (v 3.06) program. Non-linear regression was performed with SigmaPlot (v.11). Unless otherwise specified, data were presented as the means from at least three independent experiments performed in triplicate with S.E. indicated.

3.3 Results

3.3.1 Effect of anthracene-polyamine conjugates on iRBC proliferation

The effect of the anthracene-polyamine conjugates on intra-erythrocytic *P. falciparum* (3D7) parasite proliferation *in vitro* was determined using the SYBR Green I fluorescence assay. Dose-response curves indicated that the compounds have IC_{50} values in the nM range (Fig. 3.2). However, culture media has previously been shown to contain serum amine oxidases that could artificially enhance the growth inhibitory effect of polyamines and their analogues in cell cultures *in vitro* (Gahl and Pitot, 1978). Amine oxidases convert spermidine and spermine (but not the diamine putrescine) into their aldehyde forms with the resultant production of toxic NH_3 and H_2O_2, which is toxic to intra-erythrocytic *P. falciparum* parasites (Lee and Sayre, 1998; Morgan *et al.*, 1986). This can be prevented by the addition of the amine oxidase inhibitor aminoguanidine (Stjernborg and Persson, 1993). Therefore, in order to restrict the anthracene-polyamine conjugates to their polyamine form, non-toxic concentrations of aminoguanidine (0.5 mM; (O'Connell-Jones, 2009)) were included in the SYBR Green I fluorescence assays. In the presence of aminoguanidine, the IC_{50} values of the homospermidine (Ant-44 and bi-conjugated 44-Ant-44) and homospermine (Ant-444) conjugates increased at least 5-fold ($P \leq 0.05$) (Fig. 3.2 and Table 3.1), indicating that their oxidation products contributed to the low IC_{50} values observed in the initial experiments. In contrast, and as expected, the IC_{50} values of the putrescine-conjugate, Ant-4, were similar in the absence or presence of aminoguanidine (640±9 nM vs. 622±40 nM, n=9, $P \geq 0.05$, Table 3.1).

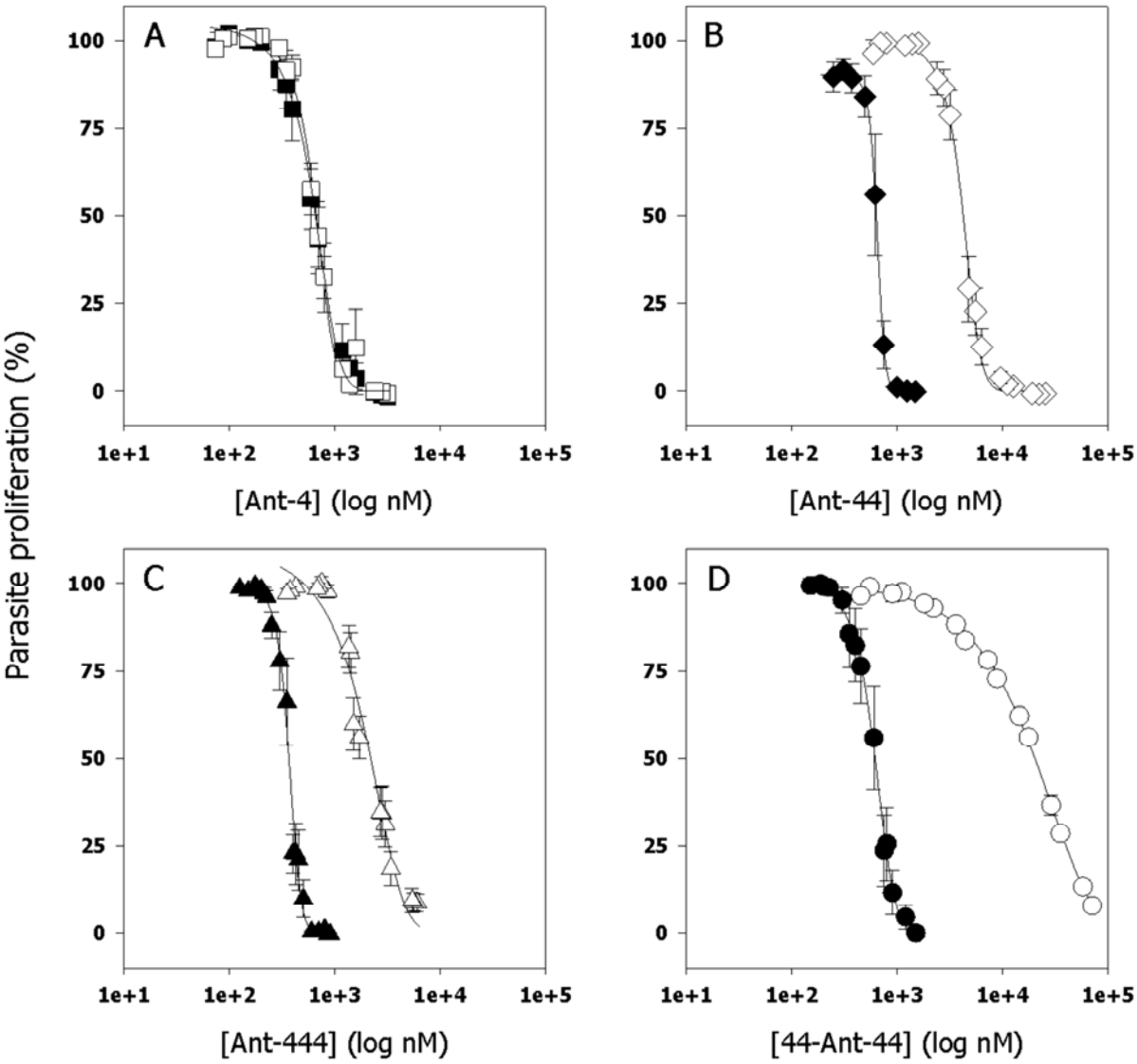

Figure 3.2: Dose-response curves showing the inhibitory effect of anthracene-polyamine conjugates on the proliferation of intra-erythrocytic *P. falciparum* parasites *in vitro* over 96 hrs (initiated with ring-stage parasites) at 37°C in the absence (filled symbols) or presence (empty symbols) of 0.5 mM aminoguanidine. The data are averaged from n experiments and are shown ± S.E. (A) Ant-4; n=9, (B) Ant-44; n=5, (C) Ant-444; n=5 and 6, respectively for the presence and absence of aminoguanidine, (D) 44-Ant-44; n=7 and 3, respectively for the presence and absence of aminoguanidine. Where not shown, error bars fall within the symbols.

To date, CHO cells are the only non-cancerous cell line for which inhibition data (IC_{50}) are available for the anthracene-polyamine conjugates (Phanstiel *et al.*, 2007). This published data were used here, together with published data for cancer cell lines (HL-60 and L1210) (Kaur *et al.*, 2008; Palmer *et al.*, 2009) to compare the selectivity of Ant-4 for intra-erythrocytic *P. falciparum* parasites relative to cancerous and non-cancerous mammalian cells. Selectivity was calculated using the selectivity index (SI) of Ant-4, which is the IC_{50}

ratio of Ant-4 against e.g. CHO cells, compared to intra-erythrocytic *P. falciparum* parasites (i.e. SI=IC_{50} CHO/IC_{50} *P. falciparum*). The SI of Ant-4 for CHO compared to intra-erythrocytic *P. falciparum* parasites was 12, indicating that Ant-4 is more toxic to intra-erythrocytic *P. falciparum* parasites than to CHO cells. This selectivity becomes more pronounced with a SI of 31 compared to cancerous HL-60 cells (Table 3.1). This selectivity of Ant-4 for intra-erythrocytic *P. falciparum* parasites compared to mammalian cells is within the accepted range of >10 for anti-malarial lead compounds (www.mmv.org). The SI values for all the other anthracene-polyamine conjugates were below 10 (Table 3.1).

Table 3.1: IC_{50} values of anthracene-polyamine conjugates against the iRBCs, CHO cells and human (HL-60) and murine (L1210) leukaemia cell lines. Intra-erythrocytic *P. falciparum* parasites were incubated with anthracene-polyamine conjugates at different concentrations at 37°C for 96 hrs (initiated with ring-stage iRBCs) and the IC_{50} values determined using the malaria SYBR Green I fluorescence assay. The rest of the IC_{50} values are from published work as indicated.

	Polyamine conjugated group[a]	IC_{50} *Pf* (nM)	IC_{50} (+AG) *Pf* (μM)	IC_{50} CHO (μM)[b]	IC_{50} HL-60 (μM)[c]	IC_{50} L1210 (μM)[d]	SI (CHO/Pf)	SI (HL-60/Pf)	SI (L1210/Pf)
Ant-4	R-putrescine	640±9 (n=9)	0.66±0.04 (n=9)	7.7	20	-	12	31	-
Ant-44	R-homospermidine	700±3 (n=5)	4.3±0.4 (n=5)	0.45	-	0.3	0.1	-	0.07
Ant-444	R-homospermine	367±19 (n=5)	1.71±0.24 (n=6)	10.6	-	7.5	6.23	-	4.4
44-Ant-44	Bi-conjugated homospermidine	627±70 (n=7)	21±5 (n=3)	1.1	-	1.5	0.05	-	0.075

[a] R indicates the anthracene conjugated moiety (Liao *et al.*, 2009)
[b] (Phanstiel *et al.*, 2007)
[c] (Palmer *et al.*, 2009)
[d] (Kaur *et al.*, 2008)
AG: aminoguanidine; L1210: mouse leukaemia cells; HL-60: human leukaemia cells; *P. falciparum* parasites: *Pf*; SI: selectivity index=ratio of the IC_{50} of Ant-4 against CHO, HL-60 or L121 cells and the IC_{50} of Ant-4 against *P. falciparum* parasites.

3.3.2 Cytostatic vs. cytotoxic effects of Ant-4

Anti-proliferative agents can be either cytotoxic, causing cell death, or cytostatic, which prevents cell proliferation and thus disease progression without actually causing cell death (Rixe and Fojo, 2007). For example, DFMO is cytostatic against intra-erythrocytic *P. falciparum* parasites, thus allowing the cells to remain viable and thereby capable of proliferation if the DFMO pressure is removed or if exogenous putrescine is provided (Assaraf *et al.*, 1987b). The malaria SYBR Green I fluorescence assay measures parasite

proliferation based on changes in DNA levels (Smilkstein *et al.*, 2004). While this assay is useful for measurement of parasite proliferation over time for IC_{50} measurements, it only measures relative DNA levels and does not distinguish between a dead cell and a viable cell capable of proliferation. The CellTiter 96® Aq_{ueous} One Solution Cell Proliferation assay (Promega, USA) is used for measuring the number of viable cells in cytotoxicity assays (Gauduchon *et al.*, 2005). This assay uses the reduction of a tetrazolium compound to a coloured formazan product by dehydrogenases to measure whether cells are viable (Cory *et al.*, 1991) and was thus used to measure the viability of Ant-4 treated intra-erythrocytic *P. falciparum* parasites (Fig. 3.3).

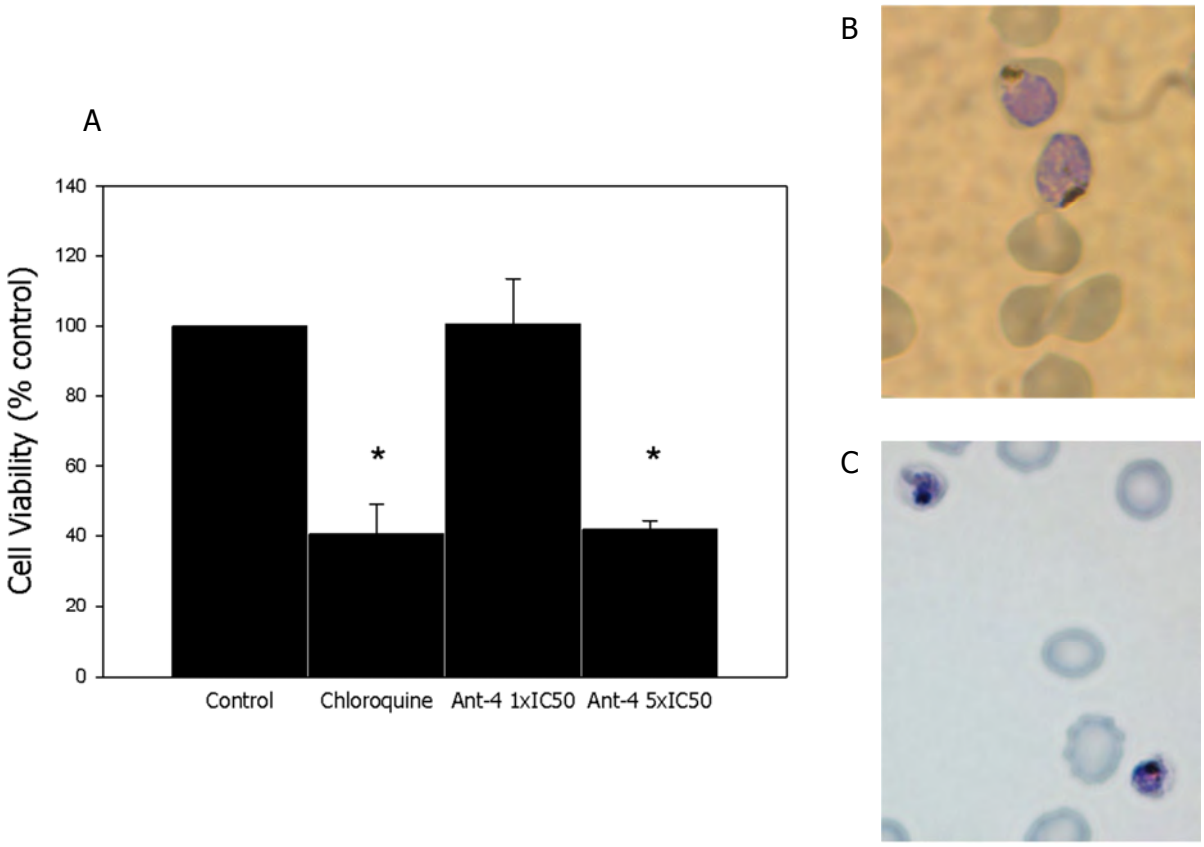

Figure 3.3: Effect of Ant-4 on the viability of intra-erythrocytic *P. falciparum* trophozoites. (A) Cell viability of trophozoite parasites was measured using the production of a coloured formazan product during 4 hrs incubation, following 24 hrs incubation of initial ring-stage iRBC cultures with different concentrations of Ant-4 at 37°C. As a positive control, chloroquine at >10xIC_{50} was used. Viability is expressed as a percentage of the untreated control cells, averaged from four independent experiments ± S.E. * $P<0.05$. (B) Untreated, trophozoite-stage Giemsa-stained intra-erythrocytic *P. falciparum* parasites. (C) Giemsa-stained 3xIC_{50} Ant-4 treated *P. falciparum* trophozoites following 24 hrs treatment at 37°C.

Ant-4 treatment caused a dose-dependent decrease in cell viability of iRBCs within 24 hrs of treatment. There was no statistically significant difference in the viability of untreated iRBCs and iRBCs treated at 1xIC_{50} ($P\geq0.05$). Treatment at 5xIC_{50}, however, showed a significant

decrease ($P \leq 0.05$) in cell viability. This decrease in cell viability was similar to that seen after treatment of iRBCs with chloroquine at a concentration of >10xIC_{50}. The Ant-4 treated trophozoites were also visibly affected, displaying the pyknotic morphology characteristic of stress-forms of the parasite (Fig. 3.3 C) (Deponte and Becker, 2004).

Parasitaemia was furthermore monitored in the presence of Ant-4 over 96 hrs using Giemasa-stained smears to determine if the cell number remains constant, indicative of a cytostatic response, or decreased due to a cytotoxic response to Ant-4 treatment of iRBCs (Fig. 3.4) (Rixe and Fojo, 2007). From 24 hrs onwards, there was a statistically significant increase in the parasitaemia of the control iRBCs compared to the Ant-4 treated iRBCs at the same time-points ($P \leq 0.05$), suggesting reduced viability of the Ant-4 treated iRBCs. Furthermore, at the end of the two lifecycles monitored, the parasitaemia of Ant-4 treated iRBCs was significantly reduced in comparison to the starting parasitaemia ($P \leq 0.05$), confirming the cytotoxic (as opposed to cytostatic) effect of Ant-4 on the parasites. In contrast to what was seen with DFMO treatment (Assaraf *et al.*, 1987b), the presence of ~500-fold excess of putrescine (compared to Ant-4) was not able to reverse the cytotoxic phenotype and restore growth of the parasites (Fig. 3.4).

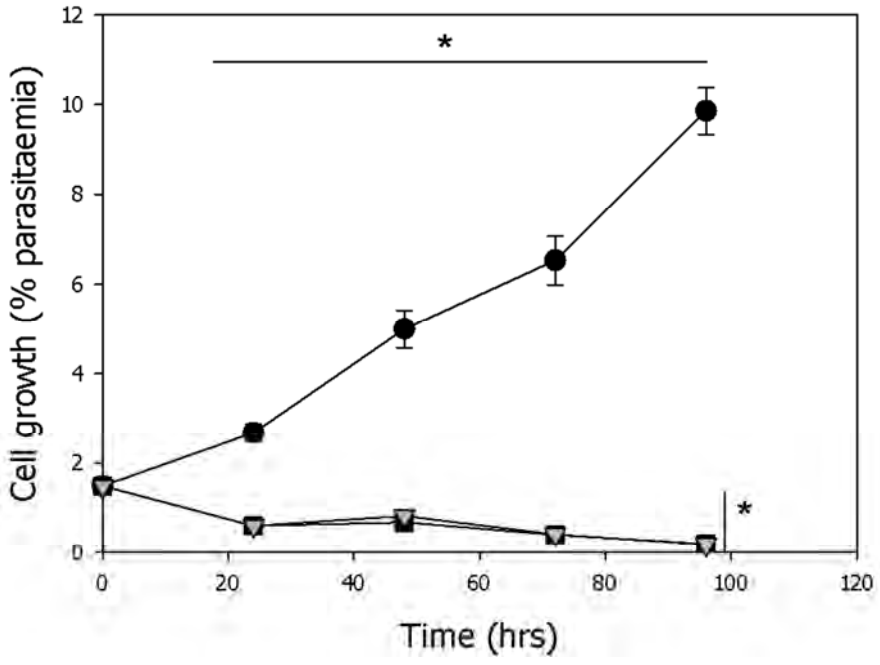

Figure 3.4: Cytotoxicity of Ant-4 against intra-erythrocytic *P. falciparum* parasites in the absence and presence of putrescine. iRBC cultures were treated with vehicle (1xPBS) for negative control (●), 3xIC_{50} Ant-4 (■) and 3xIC_{50} Ant-4 with 1 mM putrescine (▼) at 37°C and the parasitaemia monitored for 96 hrs using Giemsa-stained smears. The experiment was initiated with ring-stage parasites. Data are averaged from three independent experiments and given ± S.E. * $P<0.05$. Error bars fall within the symbols where not shown.

3.3.3 Uptake of anthracene-polyamine conjugates by iRBCs

The uptake of the fluorescent anthracene-polyamine conjugates into trophozoite-stage iRBCs was visualised with deconvolution fluorescence microscopy, using the inherent fluorescence of the anthracene moiety (excitation 364 nm, emission 416 nm) (Wang *et al.*, 2003b). Intra-erythrocytic *P. falciparum* parasites took up Ant-4, with the fluorescence localised to the parasite cytosol and nucleus (Fig. 3.5). No fluorescence was observed for Ant-4 in the RBC compartment, suggesting that there was no significant accumulation of the compound in this compartment. However, the possibility that the haemoglobin quenched the fluorescence in the RBC cannot be excluded.

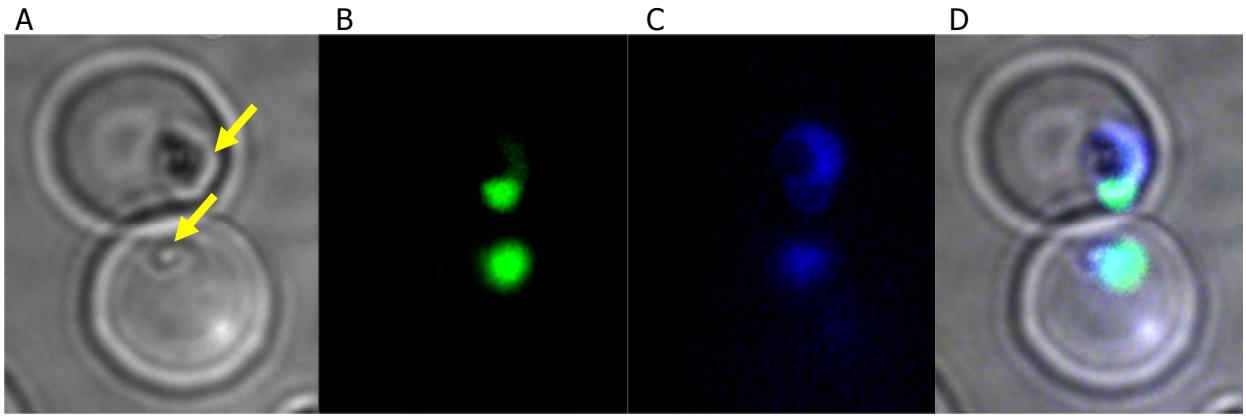

Figure 3.5: Deconvolution fluorescence microscopy of trophozoite-stage iRBCs incubated with Ant-4 (100 µM) at 37°C. (A) Trophozoite-stage parasites are visible inside RBCs in the bright-field image and are indicated with yellow arrows. Dark black haemozoin crystals are visible, particularly in the top parasite. (B) Intra-erythrocytic *P. falciparum* nuclei were visualised with SYBR Green I using a 1/1000 dilution of the commercially available stock solution and incubating the trophozoite-stage iRBCs for 1 hr at 37°C in the dark. (C) Ant-4 uptake into the trophozoite-stage iRBCs was visualised with a DAPI filter following incubation with Ant-4 (100 µM) for 1 hr at 37°C in the dark. (D) Co-localisation of Ant-4 with the *P. falciparum* parasite cytosol and nucleus.

This apparent preferential accumulation of Ant-4 in iRBCs, as opposed to accumulation throughout both iRBCs and RBCs, was confirmed with flow cytometric analyses of RBCs, iRBCs and isolated parasites incubated with Ant-4 (400 µM), with the emission measured in the DAPI channel (Fig. 3.6). There was a significant ~15-fold increase in the Ant-4 signal in iRBCs vs. RBCs (iRBCs 31.3±1.9 vs. RBC 2.1±0.2 relative fluorescence units, n=3, $P \leq 0.05$) (Fig. 3.6 A and B). Additionally, there was a strong fluorescent signal associated with the isolated *P. falciparum* trophozoites (112±9 relative fluorescence units, n=3, Fig. 3.6 C). These results are consistent with the observation made by deconvolution fluorescence microscopy: Ant-4 accumulates preferentially in iRBCs, with little uptake into RBCs.

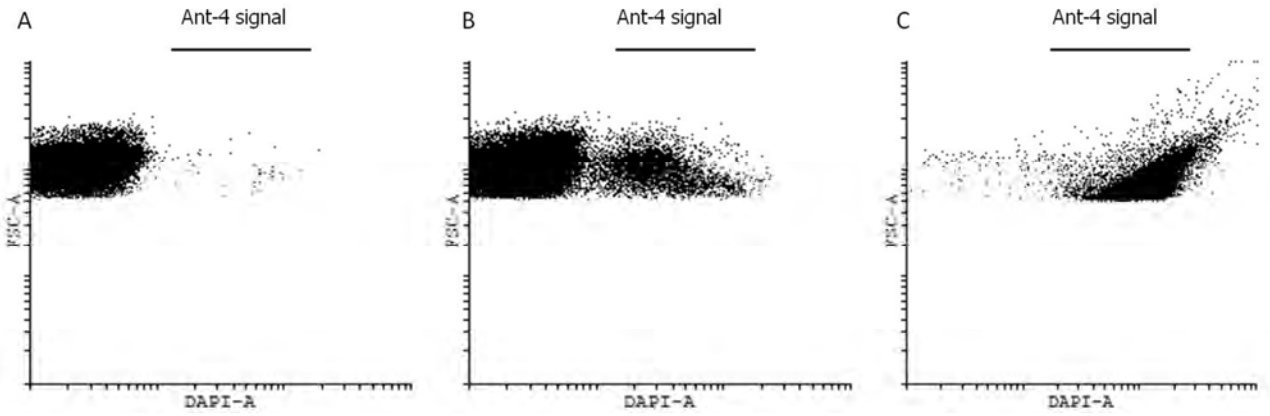

Figure 3.6: Flow cytometric scatter plots of Ant-4 signal (DAPI channel) in (A) RBCs, (B) iRBCs and (C) isolated *P. falciparum* trophozoites. The different cell suspensions were incubated with Ant-4 (400 µM) at 37°C for 1 hr before measuring the fluorescence in the DAPI channel. Results are representative of a single experiment, with data from at least 10^5 cells captured.

Pre-treatment of cancerous cells such as HL-60 and L1210 with DFMO increases subsequent polyamine uptake due to the inhibition of ODC, which causes a decrease in intracellular polyamine levels (Alhonen-Hongisto *et al.*, 1980; García-Fernández *et al.*, 2005; Walters and Wojcik, 1994). In these cells, DFMO treatment also led to a decrease in the IC_{50} of anthracene-polyamine conjugates, postulated to be due to increased uptake of the latter (Palmer *et al.*, 2009; Tomasi *et al.*, 2010). Treatment of iRBCs with the polyamine biosynthesis inhibitor DFMO results in decreased polyamine levels (Assaraf *et al.*, 1987a) and, as is the case in cancer cells, increased total putrescine uptake 2-fold and total spermidine uptake 4-fold (section 2.3.2.6). The IC_{50} of Ant-4 measured in cells pre-treated with DFMO was significantly lower than that measured in control cells (640±9 nM control cells vs. 545±17 nM DFMO-treated cells, n=3, $P \leq 0.05$) (Fig. 3.7).

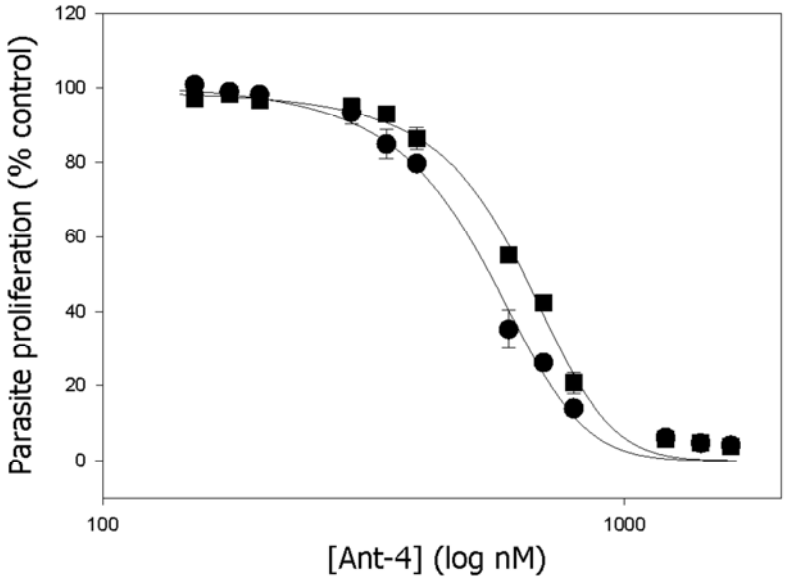

Figure 3.7: Effect of DFMO pre-treatment on the cytotoxicity of anthracene-polyamine conjugates against iRBCs, using Ant-4. Ring-stage iRBCs were incubated with (●) or without (■) 1 mM DFMO for 24 hrs, washed, and the now trophozoite-stage iRBCs incubated for a further 72 hrs with different concentrations of Ant-4 before determining the IC_{50} using the SYBR green I fluorescence assay. Data are averaged from three independent experiments and given ± S.E. Error bars fall within the symbols where not shown.

To investigate the effect of the anthracene-polyamine conjugates on the uptake of putrescine and spermidine, the inhibition of [^{3}H]putrescine and [^{3}H]spermidine uptake into functionally isolated *P. falciparum* trophozoites in the presence of the anthracene-polyamine conjugates was measured as described in section 2.2.1. The serum amine oxidases present in the culture media (present due to Albumax II) were washed away during the isolation process and thus the compounds were in their polyamine form without the presence of the oxidation products that led to the nM IC_{50} values obtained for the spermidine and spermine conjugates seen in the previous section. The putrescine conjugate Ant-4, the homospermidine conjugates Ant-44 and 44-Ant-44 and the homospermine conjugate Ant-444, all significantly ($P \leq 0.05$) reduced polyamine uptake into isolated *P. falciparum* trophozoites as measured over 30 min (Fig. 3.8). Putrescine uptake was reduced between 20% and 30% by the anthracene-polyamine conjugates (500 µM), whereas spermidine uptake was reduced by between 60% to 95%.

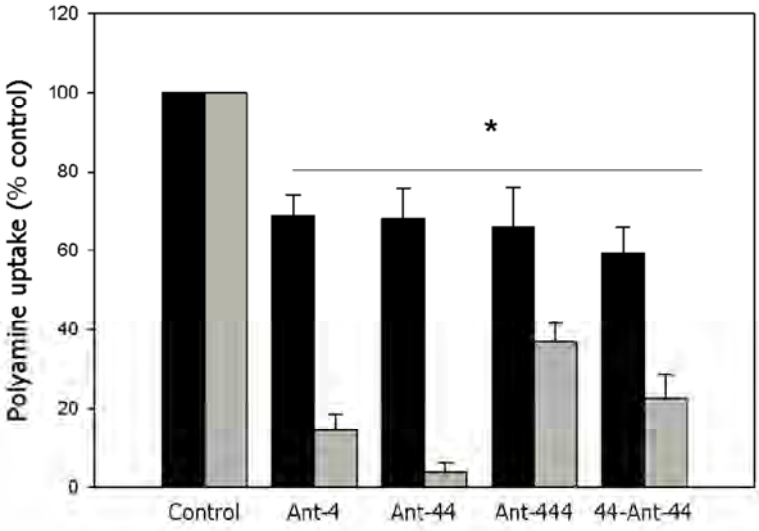

Figure 3.8: Inhibition of [^{3}H]putrescine (black bars) and [^{3}H]spermidine uptake (grey bars) into isolated *P. falciparum* trophozoites by anthracene-polyamine conjugates (500 µM) at 37°C during a 30 min incubation. For both polyamines the extracellular concentration was approximately 5 nM and the anthracene-polyamine conjugates were added to the cells simultaneously with the polyamines. All conditions are given as percentage of control (no competing substrate), averaged from four independent experiments, * $P<0.05$. [^{3}H]putrescine uptake is indicated by black bars and shown ± S.E. and [^{3}H]spermidine uptake by grey bars and shown ± S.E.

The previous result showed that the anthracene-polyamine conjugates inhibit polyamine uptake into isolated *P. falciparum* trophozoites. If these compounds enter the parasite via the polyamine uptake mechanism(s), the reverse, i.e. that polyamines reduce the uptake of the anthracene-polyamine conjugates, should also be true. The inherent fluorescence of the anthracene-polyamine conjugates, particularly Ant-4 was used with flow cytometric analyses to determine the effect of polyamines on Ant-4 uptake in iRBCs (Fig. 3.9).

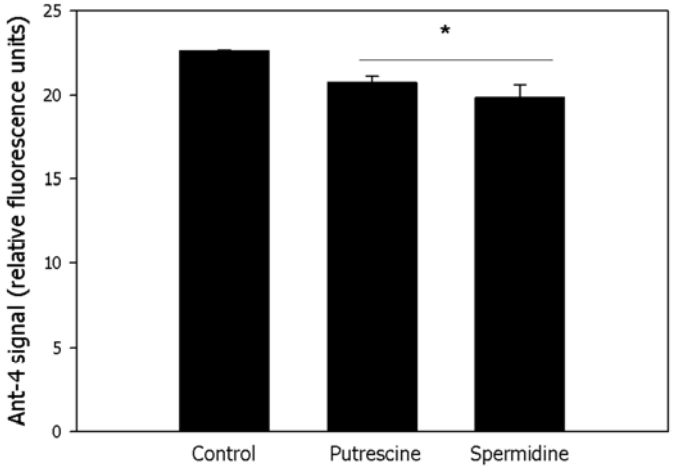

Figure 3.9: Inhibition of Ant-4 uptake (400 µM) into trophozoite-stage iRBCs by polyamines (500 µM) at 37°C following 1 hr incubation. The iRBC cultures were incubated with Ant-4 and polyamines (added simultaneously) at 37°C for 1 hr before flow cytometry fluorescence measurements from at least 10^5 cells were obtained. Results are given as relative fluorescence units, averaged from three independent experiments, * $P<0.05$, and shown ± S.E.

There was a statistically significant, albeit slight, decrease in the Ant-4 signal in trophozoite-stage iRBCs in the presence of near-equimolar concentrations of both putrescine (control 22.617±0.028 vs. putrescine 20.8±0.4, relative fluorescence units, n=3, $P \leq 0.05$) and spermidine (control 22.617±0.028 vs. spermidine 19.9±0.7, relative fluorescence units, n=3, $P \leq 0.05$).

3.3.4 Effect of Ant-4 treatment on intracellular polyamine levels in iRBCs

In contrast to what was observed with HL-60 cells (Palmer *et al.*, 2009), there were no statistically significant differences in the levels of putrescine, spermidine or spermine in iRBCs following 24 hrs of incubation with Ant-4 ($P \geq 0.05$) (Fig. 3.10), suggesting that Ant-4 treatment does not affect polyamine biosynthesis in intra-erythrocytic *P. falciparum* parasites. This lack of effect on polyamine levels of iRBCs treated with Ant-4 is supported by earlier experiments in which it was shown that Ant-4 treatment does not inhibit the activity of either ODC or AdoMetDC of *P. falciparum* (Verlinden, 2009). These results indicate that the major cytotoxic action of Ant-4 on intra-erythrocytic *P. falciparum* parasites is independent of changing the polyamine levels in the parasite.

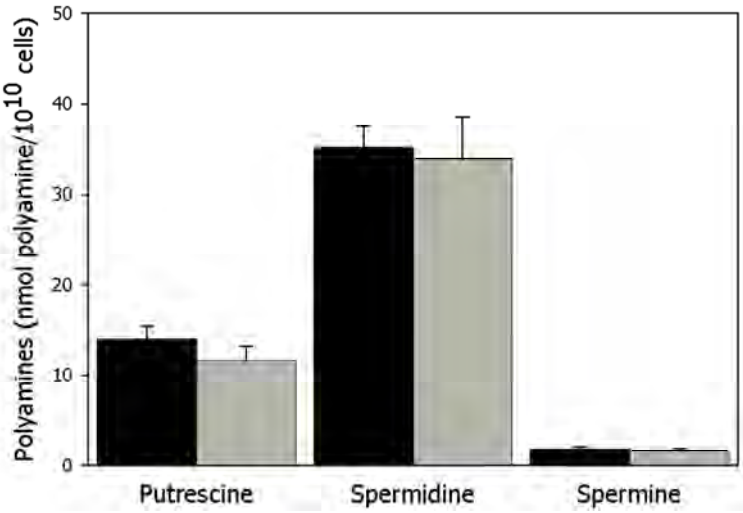

Figure 3.10: Polyamine levels of trophozoites-stage iRBCs following Ant-4 treatment. Ring-stage iRBC cultures were treated with vehicle for control (black bars) or 2xIC_{50} Ant-4 (grey bars) for 24 hrs at 37°C and the polyamines present in the now trophozoite-stage parasites extracted with PCA for 12 hrs at 4°C, followed by benzoylation for 30 min at 37°C to allow for HPLC measurement of the polyamines. Data are averaged from three independent experiments and given ± S.E.

3.3.5 Effect of Ant-4 on the reducing environment of iRBC

In HL-60 cells, Ant-4 induced cell death is postulated to be due in part to oxidative stress (Palmer *et al.*, 2009). The levels of ROS were determined with flow cytometric analyses using the fluorescent dye DCFDA that fluoresces when oxidised. In contrast to iRBCs treated with H_2O_2 as a positive control for ROS, there was no significant difference ($P \geq 0.05$) between the H_2O_2 levels in untreated intra-erythrocytic *P. falciparum* trophozoites and Ant-4 treated intra-erythrocytic *P. falciparum* trophozoites (Table 3.2).

Table 3.2: Measurement of H_2O_2 (DCFDA signal) and reduced glutathione levels as indicators for the reducing environment in Ant-4 treated intra-erythrocytic *P. falciparum* trophozoites. iRBCs were incubated with Ant-4 ($1xIC_{50}$) for 24 hrs or with H_2O_2 (20 µM) for 30 min at 37°C before incubating the untreated and treated trophozoite-stage iRBCs with 20 µM DCFDA (20 µM) for 20 min at 37°C. Flow cytometry was then used to measure the fluorescence from at least 10^5 cells. Alternatively, iRBCs were incubated with Ant-4 ($1xIC_{50}$) for 24 hrs at 37°C before using the luminescent GSH-Glo™ Glutathione Assay (Promega) to determine the concentration of reduced glutathione in the untreated and treated iRBCs. Data are averaged from n independent experiments and are shown ± S.E.

	DCFDA signal[a] (n=3)	Reduced glutathione[b] (n=4)
Untreated intra-erythrocytic *P. falciparum*	5.6±0.5	8.2±0.7
Ant-4 ($1xIC_{50}$) treated intra-erythrocytic *P. falciparum*	5.4±0.9	7.5±0.9
H_2O_2 (20 µM) treated intra-erythrocytic *P. falciparum*	86.0± 0.8	-

[a] DCFDA signal measures in relative fluorescent units,

[b] µM reduced glutathione/10^{10}cells

The presence of the reduced form of glutathione is vital for the maintenance of a reducing environment in the intra-erythrocytic *P. falciparum* cytosol (Becker *et al.*, 2003). To confirm the apparent lack of effect of Ant-4 on the reducing environment of intra-erythrocytic *P. falciparum* trophozoites, reduced glutathione levels were measured following Ant-4 treatment of intra-erythrocytic *P. falciparum* parasites. Ant-4 treatment of intra-erythrocytic *P. falciparum* parasites at $1xIC_{50}$ had no significant effect ($P \geq 0.05$) on the levels of reduced glutathione in intra-erythrocytic *P. falciparum* trophozoites (Table 3.2). This confirms that the cytotoxicity of Ant-4 to the parasite is not caused by oxidative stress.

3.3.6 Effect of Ant-4 on iRBC mitochondrial membrane potential (Δψm)

The Δψm of intra-erythrocytic *P. falciparum* trophozoites was monitored with the fluorescent, cationic dye JC-1 to determine if the cytotoxic effect of Ant-4 is due to depolarisation of the Δψm. In healthy cells with normal Δψm, JC-1 exhibits potential-dependent accumulation in mitochondria and give rise to a red fluorescence due to the concentration dependent aggregation of JC-1 (FL-2 signal, Fig. 3.11). In cells with a loss in Δψm e.g. apoptotic cells, the dye cannot enter the mitochondria and aggregate, and therefore fluoresces green (increased FL-1 signal, Fig. 3.11) in its cytosolic monomeric form.

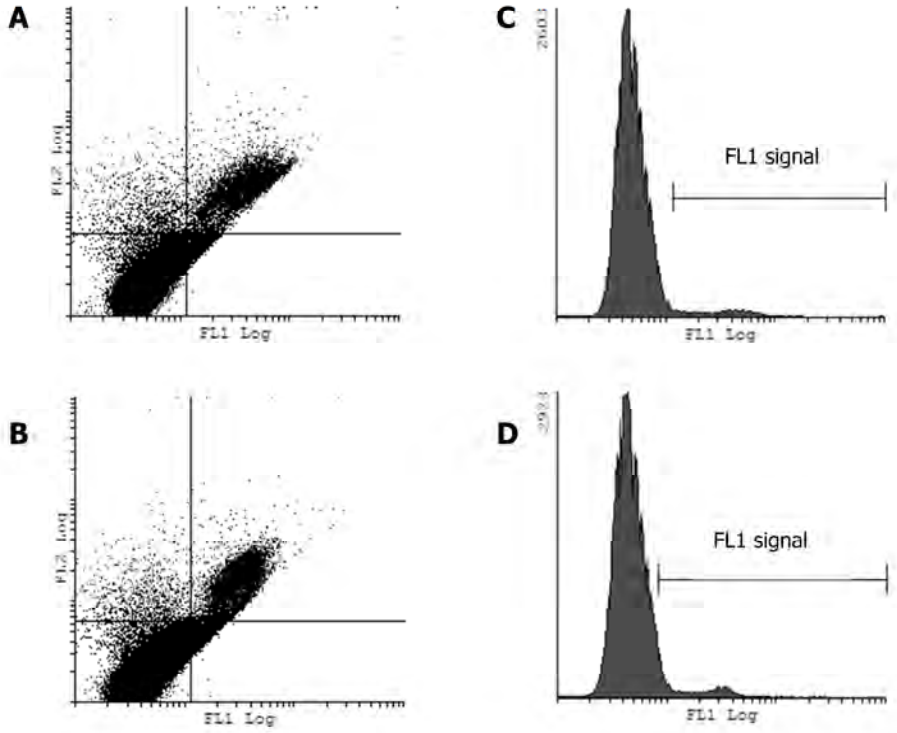

Figure 3.11: Flow cytometric profiles of JC-1 signal as indicator of changes in mitochondrial membrane potential due to Ant-4 treatment of iRBCs. Ring-stage iRBCs were incubated with Ant-4 (1xIC_{50}) at 37°C for 24 hrs before incubating the now trophozoite stage iRBCs in 1xJC-1 solution at 37°C for 15 min in the dark, and analysing 10^5 cells by flow cytometry. Scatter plots indicate the FL2 (red signal) and FL1 (green signal) channels of untreated (A) and Ant-4 treated parasites (B). Gating based on the increase in FL1 signal in the right bottom quadrants produced histograms (C) and (D), from which peak areas could be determined providing relative fluorescent units. Results are representative of a single experiment.

A 2-fold increase was observed in green fluorescence in Ant-4 (1xIC_{50}) treated intra-erythrocytic *P. falciparum* parasites compared to untreated parasites (1.24±0.12 in Ant-4

treated cells, vs. 0.63±0.03 in untreated cells, relative fluorescence units, n=2); however, this was not statistically significant ($P \geq 0.05$). This apparent loss in mitochondrial membrane potential in intra-erythrocytic *P. falciparum* following Ant-4 treatment may contribute to intra-erythrocytic *P. falciparum* cell death.

3.3.7 Ant-4 treatment affects DNA replication in iRBC

Polycyclic aromatic hydrocarbons (PAH) such as anthracene often induce DNA damage i.e. strand breaks, oxidative damage or PAH-DNA adduct formation (Cavallo *et al.*, 2008; Chakravarti *et al.*, 2008). To determine whether Ant-4 affects the intra-erythrocytic *P. falciparum* parasites' DNA replication, cells were incubated with Ant-4 ($3xIC_{50}$) and DNA levels were measured over 96 hrs using SYBR Green I fluorescence (Fig. 3.12). Following 24 hrs under Ant-4 pressure, the DNA levels in intra-erythrocytic *P. falciparum* parasites stayed constant over the two lifecycles analysed (comparison of DNA levels of Ant-4 treated parasites at t=24, 48, 72 and 96 hrs, $P \geq 0.05$), suggesting that no DNA replication occurred, compared to the significant increase in DNA levels of the control intra-erythrocytic *P. falciparum* parasites (comparison of DNA levels of untreated parasites at t=24, 48, 72 and 96 hrsas well as comparison of untreated to Ant-4 treated parasites' DNA levels at each individual time-point , $P \leq 0.05$).

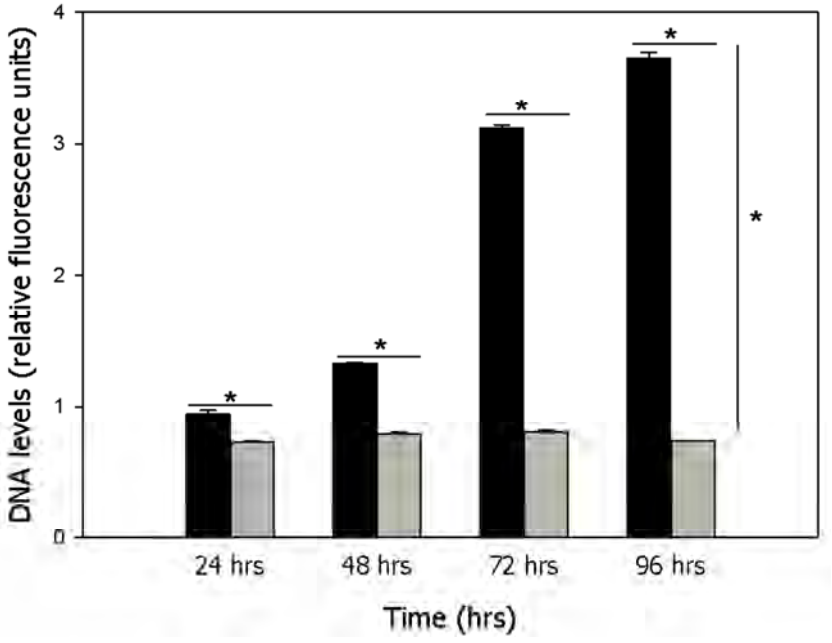

Figure 3.12: Intra-erythrocytic *P. falciparum* DNA levels following treatment with Ant-4. Intra-erythrocytic *P. falciparum* parasites were incubated with vehicle (1xPBS) for control (black bars) or $3xIC_{50}$ Ant-4 (grey bars) for the specified times at 37°C. At each time point, DNA levels were measured as relative fluorescence units following an 1 hr incubation of equal volumes of the iRBCs and SYBR Green I lysis buffer at room temperature in the dark. Data are averaged ± S.E. from three independent experiments. * $P<0.05$.

Every 48 hrs, the DNA of the intra-erythrocytic *P. falciparum* parasite replicates as the parasite develops from a single-nucleated (1N) ring stage (0 hr) and early trophozoite stage (24 hrs) to the multi-nucleated schizont stage (>2N, 36 hrs) and finally to the release of merozoites. The inhibition of DNA replication as a cause of the cytotoxic effect of Ant-4 against intra-erythrocytic *P. falciparum* was investigated by the flow cytometric profiles of the untreated and Ant-4 treated parasites over 48 hrs (Table 3.3). DNA replicated in untreated iRBCs and nuclear division occurred as expected, resulting in a reduction in the percentage of parasites with 1 nucleus (1N) and an increase in the percentage of parasites with >2 nuclei (2N) at >24 hrs. After 48 hrs, the untreated parasite again reflected a 1N ring-stage population starting their second lifecycle. Ant-4 treated intra-erythrocytic *P. falciparum* parasites exhibited a dose-dependent effect on DNA replication, with no DNA replication in parasites treated at 5xIC_{50}. In these cells, no nuclear division occurred and the parasites remained in the initial 1N stage, indicating that Ant-4 interferes with the parasite's DNA replication within the first 24 hrs of exposure.

Table 3.3: Flow cytometric analysis of nuclear division of intra-erythrocytic *P. falciparum* parasites. iRBCs (starting with ring-stage parasites) were exposed to Ant-4 (1xIC_{50} and 5xIC_{50}), or vehicle (1xPBS, negative control) at 37°C for 48 hrs and cell samples taken at 4 hrs, 24 hrs, and 48 hrs post treatment. iRBC DNA (originating from the *P. falciparum* parasite) was subsequently stained with 20 µl 1:1000 SYBR Green I for 30 min in the dark at room temperature, before measuring the fluorescence of at least 10^5 cells for each sample, with fluorescence emission collected in the FL-1 channel (FITC signal). Ring or early trophozoite-stage iRBCs contain 1 nucleus (1N), followed by nuclear division in late trophozoites (2N) and multi-nucleated shizonts (>3N). Data are averaged ± S.E. from three independent experiments**.**

		Relative percentage of cells/population				
Treatment	Hours post treatment	1N	2N	3N	4N	>4N
Control	4	88.4±0.2	3.60±0.04	0.21±0.02	0.07±0.01	0.08±0.01
	24	28.5±2.1	36.8±1.8	20.4±2.5	6.4±1.0	0.43±0.05
	48	60.5±0.5	22.0±0.6	9.9±0.5	2.7±0.1	2.6±0.1
Ant-4 (IC_{50})	4	88.7±0.4	3.2±0.1	0.12±0.01	0.06±0.01	0.05±0.01
	24	28.1±0.8	39.8±0.2	19.7±0.5	3.60±0.02	0.17±0.05
	48	54.7±0.8	18.4±0.3	7.5±0.2	3.9±0.2	12.4±1.0
Ant-4 (5xIC_{50})	4	88.7±0.1	3.5±0.1	0.1	0.03±0.03	0.03±0.01
	24	87.3±0.3	3.90±0.03	0.17±0.02	0.02±0.02	0.03
	48	74.1±0.7	8.5±1.2	0.4±0.1	0.05±0.01	0.02±0.01

3.4 Discussion

Several anthracene derivatives have been shown to have anti-malarial properties (Besley and Goldberg, 1954; Bruce-Chwatt and Archibald, 1953; Schmelzer and Gurib-Fakim, 2008; Traxler *et al.*, 1975), but in-depth analyses of the effect of these compounds on intra-erythrocytic *P. falciparum* parasites have not been performed. Additionally, a number of polyamine analogues have anti-plasmodial activity (Bitonti *et al.*, 1989; Edwards *et al.*, 1991; Klenke *et al.*, 2003). Previously, anthracene conjugated to a variety of polyamines were shown to be active against CHO (Phanstiel *et al.*, 2007; Wang *et al.*, 2003a), HL-60 (Palmer *et al.*, 2009) and L1210 cells (Kaur *et al.*, 2008). As both anthracene derivatives and polyamine analogues have shown anti-plasmodial activity, the effect of anthracene conjugated to polyamine moieties on intra-erythrocytic *P. falciparum* parasites was investigated.

An anthracene-putrescine conjugate (Ant-4) was shown to be highly active against intra-erythrocytic *P. falciparum* parasites in the nM range (Fig. 3.2), which makes it potentially interesting as a novel anti-malarial. International anti-malarial drug discovery consortia, including MMV, consider novel compounds to be attractive for further evaluation as lead inhibitors if they show activity below 1 µM (www.mmv.org). Anthracene conjugated to homospermidine and homospermine could not elicit an inhibition of parasite growth below 1 µM, making them less interesting regarding their development in therapeutic strategies against malaria. Since all four polyamine conjugates contain the same cytotoxic moiety, the differences in the inhibitory effect of these compounds on intra-erythrocytic *P. falciparum* parasites (Ant-4>Ant-444>Ant-44>44-Ant-44) can possibly be attributed to the different polyamine moieties. In the case of HL-60 cells, the putrescine moiety of Ant-4 acts as a DNA-targeting vector, delivering the anthracene moiety to DNA (Palmer *et al.*, 2009). Similarly, in intra-erythrocytic *P. falciparum* parasites, the polyamine moiety may play a crucial role in delivering the anthracene moiety to a particular effector site inside the cell, and this delivery may be polyamine-specific. Alternatively, this data may provide preliminary information on the polyamine requirements for cellular entry, with the reduced growth inhibition by homospermine and homospermidine conjugates indicating that these compounds are less able to enter the parasites.

In contrast to what was observed here for *P. falciparum* parasites, in the mammalian cell lines L1210 and CHO the anthracene-homospermidine conjugate Ant-44 was more effective in inhibiting cell proliferation than the anthracene-putrescine conjugate Ant-4 (Kaur *et al.*, 2008; Phanstiel *et al.*, 2007). This is reflected in the high SI of Ant-4 for intra-erythrocytic *P. falciparum* parasites (Table 3.1).

Ant-4 exhibited dose-dependent cytotoxicity (as opposed to a cytostatic effect) against intra-erythrocytic *P. falciparum* parasites, leading to decreased cell numbers over time (Fig. 3.3 and 3.4). Polyamine analogues may result in cell growth inhibition due to the reduction of polyamine levels through either biosynthesis inhibition or induction of polyamine catabolism and export (polyamine anti-metabolites). Alternatively, they may occupy normal polyamine binding/effector sites without performing the normal biological actions of the endogenous polyamines (polyamine mimetics) (Wallace and Fraser, 2004; Wallace *et al.*, 2003). In contrast to the situation in HL-60 cells (Palmer *et al.*, 2009), HPLC analyses showed that intra-erythrocytic *P. falciparum* parasites incubated with Ant-4 did not have decreased polyamine levels (Fig. 3.10). In addition, there is no evidence for polyamine biosynthesis inhibition in Ant-4 treated intra-erythrocytic *P. falciparum* parasites, as Ant-4 did not inhibit the activities of heterologously expressed PfAdoMetDC/ODC (Verlinden, 2009). In general, the anti-proliferative effect of polyamine biosynthesis inhibitors can be overcome with exogenous polyamines (summarised in Table 1.2). However, exogenous putrescine did not reverse the cytotoxic effect of Ant-4 on intra-erythrocytic *P. falciparum* parasites (Fig. 3.4).

There is a complex relationship between polyamines and oxidative stress. In mammalian cells, high levels of polyamines, particularly spermidine and spermine, can be catabolised to their acetylated derivatives with the resultant production of H_2O_2 (Fig. 1.5), which leads to oxidative stress and ultimately cell death (Casero and Pegg, 2009; Wallace *et al.*, 2003). However, polyamines can also protect mammalian cells (mouse fibroblasts) from oxidative stress by directly scavenging radicals (Rider *et al.*, 2007) or, in prokaryotes, by the induction of ROS-responsive transcription factors needed for transcriptional activation cascades of anti-oxidant genes (Jung and Kim, 2003). Polyamine analogues have been shown to affect the oxidation status of cells, with Ant-4 treatment resulting in reduced polyamine levels as well as increased oxidative stress in HL-60 cells (Palmer *et al.*, 2009). However, in Ant-4 treated intra-erythrocytic *P. falciparum* parasites, where there was no change in the polyamine levels (Fig. 3.10), there was additionally no evidence of a change in reductive environment of the parasite or in the production of ROS (Table 3.2).

Therefore, Ant-4 does not seem to act as polyamine anti-metabolite in intra-erythrocytic *P. falciparum* parasites since: 1) it does not affect polyamine levels; 2) it does not affect polyamine biosynthesis enzyme activities; 3) it does not affect the reductive environment within the cell, and 4) cell growth inhibitory effects could not be reversed by exogenous polyamines. One possibility is that Ant-4, due to its polyamine moiety, occupies normal polyamine effector sites non-functionally and thereby acts as polyamine mimetic. In HL-60 and L1210 cancer cells, treatment with DFMO results in depletion of intracellular polyamine levels and a compensatory increase in polyamine uptake (Alhonen-Hongisto *et al.*, 1980; García-Fernández *et al.*, 2005; Walters and Wojcik, 1994). Additionally, for these mammalian cells, a decrease in anthracene-polyamine conjugate IC_{50} following DFMO treatment was attributed to increased transport of the anthracene-polyamine conjugates, similar to what was seen for polyamines themselves (Palmer *et al.*, 2009; Tomasi *et al.*, 2010). However, no data are available in these reports on the exact transport characteristics for polyamines or the anthracene-polyamine conjugates, and an alternative explanation may be that there is increased accumulation of polyamines/polyamine-conjugates in these cells due to increased availability of intracellular polyamine binding sites following biosynthesis inhibition. DFMO pre-treatment of intra-erythrocytic *P. falciparum* parasites led to an increase in total polyamine accumulation (section 2.3.2.6) and a decrease in IC_{50} of Ant-4 (Fig. 3.7). It is possible that this decrease is due to increased accumulation of the Ant-4 within intra-erythrocytic *P. falciparum* parasites as a result of increased availability of intracellular polyamine binding sites and that Ant-4 thereby acts as a polyamine mimetic. However, the possibility that the decrease in IC_{50} of Ant-4 against intra-erythrocytic *P. falciparum* parasites is due to other unknown deleterious effects caused by the DFMO pre-treatment of these parasites cannot be excluded.

Since polyamines bind to DNA as one of its effector sites (Casero and Pegg, 2009; Wallace *et al.*, 2003), the conjugation of polyamines to anthracene (as DNA intercalator) may be particularly effective in eliciting a cytotoxic effect in intra-erythrocytic *P. falciparum* parasites. The planar, polycyclic ring structure of anthracene intercalates tightly but reversibly between DNA base pairs (Rodger *et al.*, 1995), inhibits DNA synthesis and induces DNA damage, typically due to disruption of DNA topoisomerase activity (Phanstiel *et al.*, 2000; Wang *et al.*, 2001). Anthracene and anthracene-polyamine conjugates are known topoisomerase II inhibitors (Phanstiel *et al.*, 2000; Wang *et al.*, 2001). Furthermore, the polyamine moiety of anthracene-polyamine conjugates have been shown to enhance the intercalation of anthracene through the polyamine moiety locking intercalated anthracene

into DNA major grooves by associating with the phosphate backbone (Rodger *et al.*, 1995). In intra-erythrocytic *P. falciparum* parasites, Ant-4 treatment resulted in decreased DNA levels in the parasite (compared to untreated parasites) within 24 hrs (Fig. 3.12). Additionally, intra-erythrocytic *P. falciparum* parasites were unable to replicate their nuclei after Ant-4 treatment (Table 3.3). Ultimately, this means that Ant-4 treated intra-erythrocytic *P. falciparum* parasites are unable to replicate their DNA to allow for asynchronous nuclear division, as nuclear division precedes cytogenesis (Arnot *et al.*, 2011).

Interestingly, a series of 9-anilinoacridines has been shown to inhibit the *P. falciparum* parasite's topoisomerase II, possibly by the intercalation of the acridine moiety into DNA and an interaction between the topoisomerase II and the 9-anilino side chain (Auparakkitanon and Wilairat, 2000). Furthermore, these 9-anilinoacridine derivatives also inhibited β-haematin formation (Auparakkitanon *et al.*, 2003). β-haematin or haemozoin is a non-toxic crystalline form of haem which the parasite produces in order to rid itself of toxic levels of haem released during the degradation of haemoglobin (Egan, 2008). The quinoline family of anti-malarials, including chloroquine, are all proposed to prevent haemozoin formation particularly due to their planar aromatic constituents allowing for pi-pi stacking with haem, thus preventing haem detoxification through the formation of haemozoin and thereby causing parasite death (Egan, 2006). The nM IC_{50} of Ant-4 against *P. falciparum* compared to the μM IC_{50} against CHO en HL-60 cells (Table 3.1) may thus be due to simultaneous inhibition of both DNA replication, possibly due to topoisomerase II inhibition, and haemozoin formation. It will be interesting to investigate this further.

The observed pyknotic nature of intra-erythrocytic *P. falciparum* parasites incubated with Ant-4 (Fig. 3.3) suggests that programmed cell death events might be occurring (Deponte and Becker, 2004). In addition, there was a decrease in mitochondrial membrane potential in *P. falciparum* as a result of Ant-4 treatment (Fig. 3.11). Although temporary mitochondrial membrane depolarisation may occur under conditions which are unrelated to cell death, it is often an indicator of some programmed cell death event (Kepp *et al.*, 2011). Mitochondrial membrane potential is influenced during programmed cell death events and serves in particular, as an early apoptosis indicator (Kumar *et al.*, 2008) but also of autophagy-mediated damage of mitochondria (Nyakeriga *et al.*, 2006; Painter *et al.*, 2010). Loss in mitochondrial membrane potential has been observed in drug-treated intra-erythrocytic *P. falciparum* parasites even when the death is atypical of apoptosis (Nyakeriga *et al.*, 2006) since parasites can enter a reversible, static state (Painter *et al.*, 2010).

Further investigation would be needed to determine if Ant-4 treatment of intra-erythrocytic *P. falciparum* parasites causes programmed cell death.

The molecular mechanisms of programmed cell death is poorly characterised in Plasmodia (Deponte and Becker, 2004). There are reports of apoptosis-like signatures, including stress-like morphology of cells (pyknotic forms) and the presence of metacaspases (Arambage *et al.*, 2009); however there are other reports indicating autophagy (Totino *et al.*, 2008). Apoptosis is usually characterised by morphological changes such as DNA fragmentation, cell shrinkage, membrane blebbing and the formation of apoptotic bodies (Deponte and Becker, 2004), while autophagy is a physiological cell process that degrades damaged cell components via a lysosomal pathway, often induced by ROS, DNA damage or nutrient deprivation (Kroemer *et al.*, 2010). Intra-erythrocytic *P. falciparum* parasites are not amenable to traditional methods of studying DNA fragmentation developed for mammalian cells (Deponte and Becker, 2004). Methods such as DNA laddering, terminal deoxynucleotidyl transferase-mediated dUTP-fluorescein nick end-labelling (TUNEL) assay, or single cell gel electrophoresis (Comet) assay, have inherent methodological pitfalls due to the small nuclear size (0.8-1.4 µM across) (Arnot *et al.*, 2011) and low DNA content of intra-erythrocytic *P. falciparum* parasites in comparison to the mammalian cells (Deponte and Becker, 2004). Furthermore, in contrast to mammalian cells, the entire blood stage development of *P. falciparum* parasites occurs with stage dependent DNA content. Even if synchronised cultures are used, inhibition of cell growth by drugs results in a DNA profile that is different from the control cells since, the latter parasites continue to progress through the subsequent developmental stages (Deponte and Becker, 2004).

As an example of these limitations, *P. falciparum* cultures treated with etoposide, a broad-spectrum DNA damaging agent, did not result in a positive TUNEL assay even though etoposide acts by inducing DNA damage (Nyakeriga *et al.*, 2006). Cognisant of these limitations, the Comet assay, which is based on differential migration of undamaged and nicked DNA in an electrical field (Olive and Bánath, 2006) was performed in an attempt to determine whether Ant-4 treatment of intra-erythrocytic *P. falciparum* parasites induce DNA damage, but the results were inconclusive. An alternative marker for apoptosis, phosphatidylinositol serine translocation to the outer plasma membrane is also difficult to determine in an intracellular parasite surrounded by three membrane systems (Deponte and Becker, 2004).

The fluorescent nature of Ant-4 allows its intracellular localisation to be monitored. The compound showed preferential accumulation in the parasite, with no significant fluorescence observed within the RBC cytoplasm of iRBCs or non-infected RBCs (Fig. 3.5 and 3.6). However, absence of detectable RBC fluorescence may be due to quenching of the Ant-4 fluorescence by haemoglobin. Polyamine analogues often have sufficient similarity in structure to the polyamines to enter mammalian cells via polyamine uptake mechanisms, since these uptake mechanisms are sufficiently promiscuous to recognise structurally similar compounds (Palmer and Wallace, 2010; Wallace and Niiranen, 2007; Wallace and Fraser, 2003). The anthracene-polyamine conjugates used in this study were initially designed to exploit this property of polyamine uptake mechanisms in mammalian cells, and it was found that these compounds are more active against cells with polyamine uptake mechanisms (Phanstiel *et al.*, 2007; Wang *et al.*, 2003a; Wang *et al.*, 2003b). The biochemical characterisation of the polyamine uptake mechanisms in *P. falciparum*-infected erythrocytes and in the intracellular parasite itself (Chapter 2) indicated that parasites take up both putrescine and spermidine. This polyamine uptake mechanism(s) was inhibited by a wide variety of structurally similar molecules, possibly due to competition for polyamine uptake (section 2.3.2.5). It is possible that these anthracene-polyamine conjugates are likewise taken up via the polyamine uptake mechanism in intra-erythrocytic *P. falciparum* parasites.

The anthracene-polyamine conjugates inhibit the uptake of putrescine and spermidine into iRBC by 30%-95% (Fig. 3.8). Additionally, putrescine and spermidine both reduced the uptake of Ant-4 (as measured over 1 hr) by ~10% (Fig. 3.9). There are several interpretations for these results. Firstly, these results may suggest that the anthracene-polyamine conjugates compete with the polyamines for uptake via the polyamine uptake mechanism to gain entry into intra-erythrocytic *P. falciparum* parasites, as was postulated for HL-60 cells (Palmer *et al.*, 2009). However, the data do not preclude the possibility that these conjugates inhibit the polyamine uptake mechanism of the isolated parasites without themselves utilising this mechanism for cellular entry, possibly due to structural similarity with the native polyamines. Secondly, the marginal effect of Ant-4 on putrescine uptake (and vice versa) may indicate that these compounds are not taken up via the same polyamine uptake mechanism, or that Ant-4 only partially utilise the same uptake mechanism as polyamines but may rely on additional uptake mechanisms into intra-erythrocytic *P. falciparum* parasites. Lastly, while a 1 hr incubation time was used to ensure that a signal was obtained using fluorescent cell sorting to measure Ant-4 uptake, Ant-4 uptake may already have largely equilibrated by this time, in which case any inhibition of the

initial rate of uptake of Ant-4 by the polyamines would not have been observed. It was shown that the uptake of putrescine reached a plateau within the first 15-30 min (section 2.3.2.1). Therefore, in order to confirm that Ant-4 utilise the polyamine uptake mechanism to enter intra-erythrocytic *P. falciparum* parasites, time-course analyses of polyamine uptake in the presence and absence of Ant-4 would have to be performed in order to determine whether Ant-4 affects the initial rate of putrescine or spermidine uptake (and thus transport across the membrane), and vice versa. For the study of Ant-4 inhibition of polyamine uptake using radiolabelled polyamines, as well as the study of polyamine inhibition of Ant-4 uptake, possibly based on the inherent fluorescence of Ant-4 with flow cytometric analysis, larger quantities of Ant-4 would be needed than are available at present.

In summary, this study indicates that anthracene-polyamine conjugates, particularly Ant-4, elicit a cytotoxic effect against intra-erythrocytic *P. falciparum* parasites in the nM range. This adverse effect was independent of the intracellular polyamine levels and could not be reversed by the addition of exogenous putrescine. While cytotoxicity of Ant-4 against intra-erythrocytic *P. falciparum* parasites is possibly due to the dual effect of both the polyamine moiety as well as the anthracene cargo resulting in interference with DNA replication, alternative modes of action, such as interference with haemozoin formation, remain to be investigated.